

# A low parameter tyre model for aircraft ground dynamic simulation

Wood, G. , Blundell, M.V. and Sharma, S.

**Author post-print (accepted) deposited in CURVE May 2012**

**Original citation & hyperlink:**

Poole, N. , Mo, T. and Brusey, J. (2009). Power consumption of microelectronic equipment for wireless sensor networks In Nanotechnology 2009: Fabrication, Particles, Characterization, MEMS, Electronics and Photonics (pp.534-537). NSTI.

<http://www.nsti.org/procs/Nanotech2009v1/6/M72.404>

**Copyright © and Moral Rights are retained by the author(s) and/ or other copyright owners. A copy can be downloaded for personal non-commercial research or study, without prior permission or charge. This item cannot be reproduced or quoted extensively from without first obtaining permission in writing from the copyright holder(s). The content must not be changed in any way or sold commercially in any format or medium without the formal permission of the copyright holders.**

**This document is the author's post-print version, incorporating any revisions agreed during the peer-review process. Some differences between the published version and this version may remain and you are advised to consult the published version if you wish to cite from it.**

**CURVE is the Institutional Repository for Coventry University**

<http://curve.coventry.ac.uk/open>

---

# A Low Parameter Tyre Model for Aircraft Ground Dynamic Simulation

---

## Author Contact Details:

### **G. Wood**

Faculty of Engineering, Coventry University, Coventry, CV15FB, UK  
gary.wood@coventry.ac.uk

### **M. Blundell**

Faculty of Engineering, Coventry University, Coventry, CV15FB, UK  
m.blundell@coventry.ac.uk

### **S. Sharma**

Airbus Operations Ltd, Filton, Bristol, UK  
Sanjiv.Sharma@Airbus.com

## Correspondence author:

### **M Blundell**

Faculty of Engineering, Coventry University, Coventry, CV15FB, UK  
m.blundell@coventry.ac.uk  
Tel: 02476 888924  
Mobile: 07974984398  
Fax: 02476 888272

KEYWORDS: (A) Elastomers and Rubbers, (E) Mechanical, (F) Elastic Behaviour

## **Abstract**

The work presented in this paper describes a new low parameter mathematical model representing the force and moment components generated in an aircraft tyre for use in the computer simulation of takeoff, landing and taxiing manoeuvres of an aircraft. As such the problems addressed fall in the area of ground vehicle dynamics and the modelling of the tyre presents similar challenges to those involved in modelling automotive tyres, albeit on a much larger scale in terms of the size and the loads on the tyre.

The model has been implemented in the Matlab/Simulink environment and designed to run initially with aircraft models defined by the industry standard multi-body systems program MSC.ADAMS<sup>TM</sup>.

An overview is provided of current automotive and aircraft tyre models along with a critique of the application and capabilities of these existing models for aircraft simulation. The need for a model which can be used to fit the limited range of data available for aircraft tyres, compared with automotive tyres, is also discussed.

The proposed Low Parameter Tyre Model (LPTM) uses a small set of model parameters that can be obtained without recourse to special software and can be easily manipulated to fit the model to available tyre test data. The model has been exercised and compared with two existing tyre models, using a multibody computer model of a tyre test machine and has been shown to produce improved predictions of the important forces and moments generated in a tyre contact patch when validated against test data. The evaluation at this stage is related to the tyre characteristics needed to simulate vehicle braking and cornering manoeuvres and the validation is against available test data for the lateral force and aligning moment arising due to slip angle.

## Nomenclature

ADAMS	Multi-body Simulation Package from MSC
$A_y$	Side Force Shape Factor (LPTM Tyre Model)
$A_{ya}$	Side Force Shape Factor Coefficient a
$A_{yb}$	Side Force Shape Factor Coefficient b
$C_\alpha$	Cornering Stiffness
$C_{\alpha,LPTM}$	Base LPTM Cornering Stiffness Parameter
$C_{xpt,\alpha}$	Pneumatic Trail Gradient Parameter
$C_{xpt,Fz}$	$C_{xpt,\alpha}$ Gradient Coefficient
$C_{xpt,INT}$	$C_{xpt,\alpha}$ Intercept Coefficient
EPSRC	Engineering and Physical Science Research Council
$F_x$	Longitudinal Force
$F_y$	Side/Lateral Force
$F_{y,\alpha}$	Side Force due to Slip Angle
$F_{y,max}$	Maximum Side Force for a Particular Vertical Force
$F_{y1}$	Side Force Generated Before the Critical Slip Angle
$F_{y2}$	Side Force Generated After the Critical Slip Angle
$F_{y,\alpha,1}$	Side Force Created Before the Critical Slip Angle Due to Slip Angle
$F_{y,\alpha,2}$	Side Force Created After the Critical Slip Angle Due to Slip Angle
$F_{y,TD}$	Side Force from Actual Test Data
$F_z$	Vertical Force/Normal Force
$F_{z1}, F_{z2}, F_{z3}$	Different Applied Vertical Loads on the Tyre
$k_z$	Vertical Tyre Stiffness
LPTM	Low Parameter Tyre Model
Mathworks	Software Supplier (Supplies MATLAB)
MATLAB	Data Analysis Program Created by Mathworks
MSC	Software Supplier (Supplies ADAMS)
$M_x$	Overturning Moment
$M_y$	Rolling Resistance Moment
$M_z$	Self Aligning Moment
P	Centre Point of Tyre Contact Patch
Simulink	Dynamic System Simulation Package Built into Mathworks MATLAB
V	Forward Velocity of the Wheel

$V_x$	Longitudinal Velocity of Contact Patch Centre
$V_y$	Lateral Velocity of Contact Patch Centre
WC	Wheel Centre
$x_{pt}$	Pneumatic Trail
$x_{pt,zero}$	Pneumatic Trail Intercept Parameter
$x_{pt,zero,Fz}$	$x_{pt,zero}$ Gradient Coefficient
$x_{pt,zero,INT}$	$x_{pt,zero}$ Intercept Coefficient
$x_{SAE}$	x-axis of SAE Axis System
$y_{SAE}$	y-axis of SAE Axis System
$z_{SAE}$	z-axis of SAE Axis System
$\alpha$	Slip/Yaw Angle
$\alpha_c$	Critical Slip Angle
$\gamma$	Camber Angle
$\zeta$	Tyre Vertical Damping Ratio
$\mu$	Coefficient of Friction
$\mu_{peak}$	Maximum Side Force Divided by the Vertical Force
$\mu_{vx}$	Velocity Parameter

## 1 INTRODUCTION

The need for a model that represents the physical behaviour of the interaction of an aircraft tyre in contact with the runway can be traced back to the middle of the last century when engineers and scientists began the search for mathematical theories to model the forces and moments generated in the tyre to runway contact patch. Those early efforts were driven by a phenomenon known as wheel shimmy, often manifested as a violent and sudden vibration in the nose landing gear on landing. The challenge to understand the contribution of the tyre in the context of wheel shimmy received considerable attention from the researchers of the time at the NASA (North American Space Agency) Langley Research Centre and resulted in seminal publications by Smiley and Smiley and Horne [1,2]. The Smiley and Horne paper [2], *Mechanical Properties of Pneumatic Tires with Special Reference to Modern Aircraft Tires (NASA Technical Report NASA-TR-64)* is still, almost 50 years later, widely regarded for the authority of the work presented, to the extent that the model described there is still commonly referred to, using the NASA report reference number, as the R-64 model.

Tyre modelling is important in a modern virtual engineering environment where it is now common practice, in both the automotive and aerospace industries, to make use of computer programs utilising a multibody systems approach to model and simulate ground vehicle dynamics and in particular the handling performance of a vehicle. It should be noted that in this paper the behaviour of an aircraft when in contact with the runway, during landing, takeoff or taxiing, is considered to be a vehicle dynamics problem.

For automotive applications the use of simulation tools has become firmly established over the last two decades and computer models are now widely used in the design and analysis of a vehicle well ahead of any work with prototype vehicles in the laboratory or on the proving ground. The software used for such purposes now falls broadly into two camps; programmes which are specifically aimed at vehicle dynamics applications such as Carsim, Carmaker or VDyna and programmes which are regarded as general purpose multibody codes, such as MSC.ADAMS or Simpack. The general purpose codes can handle a wide range of mechanical simulation applications in addition to having vehicle dynamics capability and as such have more common use in both the automotive and aerospace sectors. It should be also noted that modelling and simulation tools such as Matlab/Simulink can also be used directly to model vehicle dynamics and are most suitable for control applications where

detailed modelling of mechanical systems, suspension linkages and the like, are not included. Another mode of operation, as in the work described here, is to use Matlab/Simulink and a general purpose multibody programme together.

MSC.ADAMS is the multibody systems programme used to support the work presented in this paper and in the automotive industry is commonly used, for vehicle dynamics and a range of other applications, to represent the various subsystems comprising the suspension linkages, springs and dampers, anti-roll bars, powertrain and vehicle body. The growing use of computer simulation in the last two decades has led to derivative programs such as ADAMS/Car<sup>TM</sup> and ADAMS/Chassis<sup>TM</sup> that offer customised screen layouts facilitating the rapid construction of a model and subsequent simulation of laboratory and proving ground test procedures. The outputs from the simulations of the full vehicle allow a graphical animated presentation of the vehicle trajectory and the plotting of graphs showing time histories for the vehicle responses including, for example, lateral acceleration, body roll angle and yaw rate. As such these derivative programmes fall into the same specialist class of vehicle dynamics software as Carsim, Carmaker and VDyna.

Before a vehicle dynamics computer simulation can be performed the tyre force and moment characteristics must be estimated, predicted or obtained from experimental tests using laboratory based test machines, such as the High Speed Dynamics Machine, used for automotive tyres, formerly located at the Dunlop Tyres Research laboratory in the UK and illustrated here in Figure 1.

Using a tyre test machine, it is possible to measure the resulting force and moment components generated due to the distribution of pressure and stress in the contact patch for various camber angles, slip angles and a range of values for the vertical force. It is also possible to drive or brake the tyre and measure the forces generated due to longitudinal slip. It should be noted that complex simulations that aim to map a full range of behaviour involving combined driving or braking with cornering require more tyre model parameters and will require an extensive and expensive programme of tyre tests to be performed.

The use of nonlinear finite element methods and programmes such as Abaqus 6.1 (Dassault Systemes) to develop predictive models of tyre behaviour is also evolving and can be used to investigate, for example, the behaviour in the tyre contact patch. An example of

such a study is the work by Gruber [3] where a detailed study of the friction and camber influences on the static stiffness properties of a racing tyre is presented. Other reasons why models of this type can be considered useful are to support the delivery of design targets aimed at reducing weight while improving the structural performance of the tyre or using the model to predict in detail the transfer and distribution of load to the supporting wheel structure. The modelling and simulation challenges for a component as structurally complex as a tyre, whether automotive or aircraft, are considerable and a detailed treatment of this subject area is outside the scope of this paper.

For the applications considered in this paper a finite element model of a tyre would be of most use in providing a virtual test facility capable of simulating an equivalent programme of tests, as required in a laboratory test facility, to deliver the model parameters used, typically in empirical models, for vehicle dynamics simulations. A more detailed consideration of models used at this stage follows in section 2.

For the existing empirical tyre models, the model most established and used is the Magic Formula or MF tyre model resulting from the widely recognised work of Pacejka and his associates [4-6]. The MF tyre model is known to give an accurate representation of measured tyre characteristics, is internationally accepted and applied widely by both industry and academia. The model formulation uses modified trigonometric functions to represent the shape of curves, generally resulting from a programme of tests, representing the tyre forces and moments as functions of either longitudinal slip for tractive forces or slip angle for lateral forces and aligning moments. The complexity of the model and the simulation being addressed do however mean that a large number of model parameters may be needed, depending on the simulation to hand, to define the tyre model. This generally means that specialised software must be obtained or developed to derive the parameters from the measured test data.

A more basic and easily obtainable representation of the tyre force and moment characteristics is provided by the Fiala tyre model, which although generally used in automotive applications was first presented for consideration with aircraft tyres [7, 8]. This model also uses an empirical formulation to represent the tyre force and moment characteristics and although not capable of the accuracy obtainable from the Magic Formula, has the advantage of requiring only 10 parameters, the physical significance of which are easy



to comprehend. The parameters can also be easily and rapidly obtained from the measured tyre test data with no requirement to use special software. The drawback is that this model is not suitable for combined braking and cornering and has other limitations including; an inability to model camber thrust, a lack of load dependence in modelling cornering stiffness and the inability to model offsets in lateral force or aligning moment at zero slip angle due to plysteer or conicity.

Before a more detailed consideration of the tyre modelling subject, it is necessary to consider the scale of the problem in capturing data to support the mathematical representation of an aircraft tyre. While for automotive applications a test programme covering vertical loads in the range 2kN to 8kN and slip or camber angles up to 10 degrees is typical, the operating conditions for an aircraft tyre are far more extreme. For the aircraft tyre model discussed in this paper, loads of up to 300kN and tyre yaw (slip) angles of up to 90 degrees were considered as representative of the conditions that can occur during take off, landing and taxiing manoeuvres for a large aircraft. The image shown in Figure 2, taken in the Airbus laboratories at Filton, is included here to illustrate the sheer size of the tyres. Aircraft tyres on this scale are simply too big to be accommodated by most tyre test facilities normally used for automotive tyres.

In order to test tyres on this scale specialised facilities are required such as the NASA Installation used by Daugherty [9]. For the work described here, access to test results from the Airbus tyre test machine (Figure 3), TERATYRE, was available and provided the data resource for model validation.

## 2 TYRE TESTING AND MODELLING

The testing of aircraft tyres presents a unique demand upon the capabilities and capacities of suitable test facilities when considering the information relating to ground handling scenarios. With the increase in size and demand for various modern aircraft, the requirement for understanding the boundaries of the ground interactions and responses of tyres has also increased. As such the extended performance requirements of aircraft tyres compared with automotive tyres is significant. An example of this can be seen with the recent Airbus A380 which shows that the tyres for this aircraft (sizes for the nose and main gear are 1270x455 R22 and 1400x530 R23 respectively [11]), are far larger than normal automotive tyres and this is extenuated by the loads and operational conditions that they have to support (examples of the rated load for the two tyres are 244kN and 334kN [11]). This extended requirement for larger tyres presents a unique scenario when considering the test facilities involved in the process.

There are currently a number of facilities which can test aircraft tyres and they all have various capacities when generating the required data. NASA's Langley site is one such example where various test programmes have been employed to engage in a variety of different studies (examples from Tanner et al and Daugherty [12-14]). The test facility can replicate speeds up to 253mph, impose vertical loads up to 289kN and generate slip angles up to 15° [15]. This has been supported further with the creation of a flying test bed where a Convair 990 was modified to carry an extra landing gear so that an additional tyre could be tested and examined during actual operational conditions. This test bed had the capacity to replicate speeds up to 264mph, exert vertical loads of up to 668kN and produce slip angles up to 15° [16]. Other facilities which are utilised are stationary dynamometers such as those from Bridgestone and MTS [17, 18]. These dynamometers can normally reach the desired vertical loads when testing aircraft tyres. However, they are normally limited to 20-30° of slip angle generation which is around a third of the overall value required. More recently the ability of current test beds has been extended through the work being conducted at Airbus [10]. Figure 3 shows an example of the test rig which is called the TERATYRE. The whole rig can move and test the tyre along curved and linear trajectories. This produces much higher slip angles than normal dynamometers, but as the entire rig is moving with the tyre it has a limited speed capacity.

The scenario of a low parameter tyre model for initial simulations of the handling characteristics specifically for aircraft applications has previously been described where the resultant principal forces and moments for the tyres are replicated. These are based upon the results which are generated through various test facilities, examples of which have been described here. These test facilities all have their limitations because of the extremes in operational conditions which need to be replicated. This means that there are areas of aircraft tyre operation, as illustrated in Figure 4, which are difficult within the current knowledge to fully replicate, through testing requiring engineers to draw on the use of lineage, simulation tools and modelling.

The role and type of tyre testing is of the utmost importance when determining the capability of any tyre model. The roles and variety of tyre models to predict the outputs of a tyre for a number of scenarios will inherently require an extensive range of data in order to understand the mechanisms involved to the level required to generate responses which are accurate for a range of operational conditions. This requirement has led to a variety of tyre models being created which meet the needs of various applications. The current availability of data means that empirical based models have boundaries through which uncertainty will be generated due to difficulties in validation provided by the lack of test data. Physical tyre models however have the provision to provide a unique insight into the detailed workings of the tyre at macro and microscopic levels which can result in some of these uncertainties being answered.

Models specifically for handling and dynamic cases along with physical and durability models all have their own unique area of application. However, crossing these boundaries to unify the models creates an extremely high demand on the amount and accuracy of the data involved (be it for various forms of material or full tyre testing). Incorporating into this the wide ranging applications of tyres and the operational boundaries means that the complexity of the models increases rapidly. Table 1 provides a summary relating to the scenario surrounding tyre models which could be utilised through environments such as multibody simulation packages. For a more predictive model at a basic level, levels the complex replication of the internal structure of a tyre is needed. Over the past few decades the exploitation of computer aided engineering and principally multibody and finite element analysis packages have seen the detailed and predictive capability for modelling tyres reach significantly high levels of complexity.

A good example of a multi functional tyre model is FTire which uses the bases of a flexible ring and belt element incorporating a number of components to make it both suitable for multi-body and finite element simulation. The model comprises a number of radial elements consisting of springs and spring dampers to represent components of radial and tangential stiffness. This is further extended by the addition of a number of point masses on the outer radius to represent the belt elements which are interconnected to account for the radial, lateral and tangential movements of the belt through the use of tyre belt and bending stiffness (further details are given by Gipser [19, 20]). This integrated approach allows the model to be used successfully in ride, handling and durability studies for high and low frequency responses and for high or low wavelength obstacles. This model can determine both the in plane and out of plane dynamics of the tyre for a variety of different scenarios.

Physical tyre models have expanded from the low to high frequency capability along with in and out of plane dynamics to evaluate the scenarios of vibration and shear states within the tyre. These areas are continually being researched, refined and expanded upon to extend the understanding and responses of the models for modal and shear force generation which is paramount to determining the performance of the tyre. Brush models like the widely known Sharp model [21] to more recent accounts such as Tsotras and Mavros [22, 23] show that the work continually expands and refines these models with ever increasing complexity due to the advancements in computation power which is available. Models which incorporate both scenarios start to significantly push the computational demands due to the increase in required elements such as beam or truss based elements.

Alternative views of the physical models being employed and gaining complexity arise through the finite element method/analysis. Again as the software and hardware for these applications has increased so has the demand to understand the particular properties and construction of the tyres involved (examples of a typical tyre and wheel construction within an FEA package can be seen in Figure 5 which is from work being conducted at Coventry University). The modelling capabilities stemming from one, two and three dimensional analysis hinges on the availability or determination of the data relating to the detailed tyre material properties and construction. Determining the geometric and material properties of tyre carcass components (such as the tread, sub tread, under tread, sidewall, apex, clinch, bead, bead wrapping, inner liners, multi-layered ply's, breakers and cushions strips) requires detailed treatment before modelling can commence. Recent work such as that carried out by

Yang [24] highlights this complexity when having to determine such characteristics as the rubber material's hyperelastic and viscoelastic properties (determined through uni-axial tension tests and modelling in a CAE package) and the reinforcement elastic modulus properties (determined through a Dynamic Mechanical Analysis). This process highlights the number of properties which need to be ascertained along with selecting the appropriate modelling approaches (such as a suitable elastomeric strain energy function like those of Ogden, Gent and Arruda-Boyce) to be able to replicate the responses of the tyre accurately. Some other examples of the employment and practicalities of work in this area can be seen in Ojala and Alkan [25, 26]. This increasing interaction between the various material layers in the tyre along with the considered interaction of linear and nonlinear elements is pushing the boundaries of analysis involved, the level of material properties required and the elements which will subsequently replicate them within the simulation environment. The employment and precision of these simulations depends upon the boundary conditions being used and the particular type of output being explored.

To maintain pace with the continuing development of new technologies and material implementation within the tyre industry, it is desirable that all varieties of tyre models can be utilised in the design and development cycle. Each has an important part to play in the role of development but the boundaries through which they are employed are continually changing to meet the current needs of the industries employing them.

In automotive vehicle dynamics, early attempts to represent the tyre with a full vehicle in a multibody simulation made use of the raw tyre test data where the measured data was set up in tabular form and interpolated during the computer simulation. Interpolation methods are not useful however for investigations involving variations in tyre parameters, such as cornering stiffness, and hence mathematical models have evolved to aid design studies where the tyre is considered together with the vehicle. Advances in tyre modelling have led to empirical models that are used to fit equations to the measured test data. The quality of the model will be a compromise between accuracy, the relevance of the parameters and the availability of methods to generate the parameters. In addition to the finite element based models discussed earlier, models which are more useful for vehicle dynamics studies have also been developed using a physical representation of the tyre, such as FTire [27]. These models tend to be more useful for off road applications investigating vehicles traversing

uneven terrain and or durability studies simulating tyre impacts with road obstacles such as potholes and kerbs.

An initial objective for the work described in this paper was to review a range of tyre models used specifically for automotive or aircraft applications and models initially developed for automotive applications but adapted for aircraft. Table 1 provides a summary of some of the most popular models which are currently being widely utilised.

It can be seen that there is a distinct shortage of models which have been specifically designed for the purpose of replicating the responses of an aircraft tyres. From this review it was also found that for aircraft applications, one of the most comprehensive models is the NASA R-64 model [2]. As discussed earlier, this model was created in the 1960's and is based on small bias-ply tyres available at the time. Modern bias-ply aircraft tyres, along with increasingly utilised radial tyres, are significantly different in size and construction thus limiting the model's capability to represent modern aircraft tyres. This model has been subject to further development utilising modern aircraft tyre test data and adapting the original model to increase its capability through the work of Daugherty [9] and Tanner et al [36].

Despite this work, it is clear from Table 1 that aircraft simulation engineers are faced with a distinct lack of choice of tyre model, compared with their automotive counterparts, particularly in being able to select the model most suitable for a given application or a model which will be most robust for the test data available. The last point here is highly relevant given the difficulties involved in making available aircraft tyre test data for the wide range of conditions that occur in service. From this, a need can be clearly identified for an aircraft tyre model that can capture the main tyre contact patch force and moment characteristics from a limited range of data and provide a platform to which capability can easily be added as more data becomes available.

The starting point for the modelling work described in this paper was to consider the performance of the Fiala and Harty tyre models to represent the available aircraft tyre test data, both models being identified as having a low number of model parameters that could be obtained from a limited range of data. For automotive work, the Harty model was already considered to overcome some of the limitations of the Fiala model, particularly in the

representation of self aligning moment. The main features of the model as described by Blundell and Harty [32] include:

- Use of an empirical representation of tyre properties
- Use of a simplified implementation compared with the Magic Formula
- Inclusion of a more complete implementation than the Fiala tyre model
- Production of faster solutions
- Provision of robustness for prolonged wheel spin and low grip conditions
- Capability of modelling comprehensive slip for combined cornering and braking
- Modelling of the dependence of cornering stiffness on tyre load
- Inclusion of camber thrust

The Harty model was implemented in MSC.ADAMS using a Fortran subroutine. In MSC.ADAMS a subroutine interface known as a Tirsab is provided for users to modify and integrate their own tyre models with the main code. An example listing for an earlier nine parameter version of the Harty Tyre Model in this format is provided by the authors in Blundell and Harty [37].

For simulation on a flat road surface or runway, the function of the tyre model is to represent the forces and moments occurring at the tyre to road contact patch and resolve these to the wheel centre and hence into the vehicle or aircraft. For the model developed here, the forces and moment at the tyre to road contact patch are formulated using the SAE tyre coordinate system shown in Figure 6, where the slip angle  $\alpha$  and camber angle  $\gamma$  are presented as positive. The forces and moments calculated can include:

- $F_x$  - longitudinal tractive or braking force,
- $F_y$  – lateral (side) cornering force,
- $F_z$  - vertical normal force,
- $M_x$  – overturning moment,
- $M_y$  – rolling resistance moment,
- $M_z$  - aligning moment.

Note that in aircraft engineering the term side force is normally used for lateral force. The overturning moment  $M_x$  and the rolling resistance moment  $M_y$ , can be included if they are considered significant for the particular analysis. Both of these moments occur due to the vertical force in the actual tyre being offset from the tyre model contact point P. For automotive applications the rolling resistance is important for fuel economy. For aircraft, the overturning moment is of more significance and was considered in the work by Smiley and Horne [2] to result from lateral movement of the contact patch relative to the wheel plane due, to both slip and camber angle.

For both the Fiala and Harty models the tyre test data in the form of measured side (lateral) force and self aligning moment with slip angle was taken at three values of vertical loads ( $F_{z1}$ ,  $F_{z2}$ , and  $F_{z3}$  are different vertical loads applied to the tyre to represent the operational range of the tyre) and used to directly obtain model parameters. At this stage, the model formulations were programmed into an Excel spreadsheet to investigate the model fit to test data. For the two models the comparisons with test data for plots of lateral force with slip angle are provided in Figures 7 and 8, while plots of self aligning moment with slip angle are provided in Figures 9 and 10.

From the graphs it can be seen that for the representation of side force, the performance of the Fiala and Harty models are broadly similar with a good representation of cornering stiffness at close to zero slip angle and good agreement across the range of slip angles at the lowest load. For the self aligning moment, the Harty model performs better than the Fiala model but for both models the match with the test data requires development across the range of load and slip angle.

In developing a low parameter aircraft tyre model, areas such as the load dependency of the cornering stiffness, the onset of the peak side force along with the maximum self aligning moment and its intercept with the horizontal axis were amongst those immediately identified as requiring attention.



### 3 LOW PARAMETER TYRE MODEL

From the study described in the previous section it was seen that significant changes would be needed to create a model which could accurately replicate the aircraft tyres responses. The Harty model was utilised as a base to examine these relationships; however considerable modifications and development were required before the model was capable of accurately replicating aircraft tyre test data. As a result the new tyre LPTM tyre model (Low Parameter Tyre Model), was created and what follows is a description of how the model replicates the side force (also known as the lateral force) and self aligning moment of an aircraft tyre. Only the side force and aligning moment were fully investigated as test data for braking was not available. Modelling the rolling resistance was not considered essential at this stage and data for overturning moment was not available.

The LPTM model uses the 17 parameters listed below:

- $\alpha_c$  Critical Slip Angle
- $A_y$  Side Force Shape Factor
- $A_{ya}$  Side Force Shape Factor Coefficient a
- $A_{yb}$  Side Force Shape Factor Coefficient b
- $C_{p\alpha}$  Cornering Stiffness Parameter
- $C_\alpha$  Cornering Stiffness
- $C_{\alpha,LPTM}$  Cornering Stiffness of Base LPTM Model
- $\mu$  Coefficient of Friction
- $\mu_{vx}$  Friction due to Velocity
- $k_z$  Tyre Vertical Stiffness
- $\zeta$  Vertical Damping Ratio
- $C_{xpt,\alpha}$  Pneumatic Trail Gradient Parameter
- $C_{xpt,Fz}$   $C_{xpt,\alpha}$  Gradient Coefficient
- $C_{xpt,INT}$   $C_{xpt,\alpha}$  Intercept Coefficient
- $x_{pt,zero}$  Pneumatic Trail Intercept Parameter
- $x_{pt,zero,Fz}$   $x_{pt,zero}$  Gradient Coefficient
- $x_{pt,zero,INT}$   $x_{pt,zero}$  Intercept Coefficient

The significance of these parameters will become clear in the following discussion outlining the formulae used for each of the tyre force and moment calculations. The side force ( $F_y$  also known as the lateral force) representation is provided through the utilisation of an exponential function to generate the overall shape of the response along with a number of parameters to control the overall result inline with the trends seen within the aircraft tyre test data. To achieve this end, the side force response was broken down into three main components which could be seen to govern the relationship; these are summarised within Figure 11. Controlling these factors and accounting for vertical load effects was paramount in determining an accurate and flexible model.

Consequently these factors were factored into the main equation so that the responses could be controlled in the desired manner. This was ultimately achieved by utilising two equations which governed the side force generation. The first equation ( $F_{y\alpha,1}$ ) covers the response up to the critical slip angle ( $\alpha_c$ ), this being the point at which the maximum side force is first observed; then the second equation ( $F_{y\alpha,2}$ ) governs the response past this point. The two overall side force equations along with their boundary conditions can be seen in Equations 1 and 2 along with the slip angle ( $\alpha$ ) calculation shown in Equation 3.

$$\text{For } \alpha < |\alpha_c| \text{ then: } F_{y, \alpha, 1} = (1 - e^{-(C_{pa} + A_y)(\alpha / \alpha_c)}) \mu F_z \text{ SIGN } (-\alpha) \quad (1)$$

$$\text{For } \alpha > |\alpha_c| \text{ then: } F_{y, \alpha, 2} = (1 - e^{-(C_{pa} + A_y)\alpha_c}) \mu F_z \text{ SIGN } (-\alpha) \quad (2)$$

$$\alpha = \arctan\left(\frac{V_y}{V_x}\right) \quad (3)$$

The overall magnitude of the side force is controlled by the vertical force ( $F_z$ ) and the coefficient of friction ( $\mu$ ). The original method of calculating the vertical load is determined using a linear representation factoring the vertical stiffness with the vertical displacement of the tyre contact patch and a tyre damping coefficient factored with a rate of change of tyre vertical displacement. This was then extended using a polynomial to represent the nonlinear vertical force-displacement behaviour of the tyre characterised by testing. The coefficient of friction has also been modified to introduce dependency on vertical load and longitudinal velocity. This relationship can be seen in Equation 4 where  $C_1$  is a coefficient which is determined for the particular tyre according to the rate of change of coefficient of friction with

vertical load. The longitudinal velocity is accounted for through the velocity parameter ( $\mu_{vx}$ ) which accounts for the way in which the relationship between the coefficient of friction and longitudinal velocity changes the intercept value of the response.

$$\mu = C_1 F_z + \mu_{vx} \quad (4)$$

The critical slip angle ( $\alpha_c$ ) is the point at which the initial onset of the maximum side force occurs. The relationship can be seen in Equation 5 where the coefficients  $C_2$  and  $C_3$  relate to the gradient and intercept values of the resulting equation applied to the critical slip angle versus vertical load relationship.

$$\alpha_c = C_2 F_z + C_3 \quad (5)$$

The final two parameters for the side force equation relate directly to controlling the gradient change of the response up to the critical slip angle. The cornering stiffness parameter ( $C_{pa}$ ) relates directly to the cornering stiffness ( $C_a$ ) of the tyre, i.e. the initial gradient of the response of a side force versus slip angle graph. This parameter controls the gradient of the initial response and has been created to be load dependent. The side force shape factor ( $A_y$ ) then works in conjunction with the cornering stiffness parameter to govern the rest of the response up to the critical slip angle to ensure that a continuous change between the two side force equations is achieved. This relationship is found by reverse calculating the gradient relationship by rearranging the side force equation and inputting the test data to it. The resulting relationship delivers the base side force shape factor which can be split into the two parameters of interest, i.e. the cornering stiffness parameter and the side force shape factor.

Using the side force shape factor relationship, the initial values of the response can be used to control the cornering stiffness parameter. This is achieved by taking the cornering stiffness and dividing it by the LPTM cornering stiffness ( $C_{a,LPTM}$ ); this relationship is shown in Equation 6. The LPTM cornering stiffness is found by reversing the relationship seen within Equation 6 and inputting the known test data so that it acts as a base from which the actual cornering stiffness can be controlled.

The rest of the base side force shape factor response can then be used, minus the effects of the cornering stiffness parameter, to determine the side force shape factor which

will then control the rest of the gradient change; this relationship can be seen in Equation 7. The relationship is controlled by two coefficients  $A_{ya}$  and  $A_{yb}$  which are determined from the base side force shape factors.

$$C_{p\alpha} = \frac{C_{\alpha}}{C_{\alpha,LTPTM}} \quad (6)$$

$$A_y = A_{ya} e^{(A_{yb} |\alpha|)} \quad (7)$$

The self aligning moment ( $M_z$ ) formulation for the LPTM tyre model is based upon the side force multiplied by the pneumatic trail ( $x_{pt}$ ); this relationship is shown in Equation 8. Therefore it was assumed that if an accurate side force calculation can be generated then an accurate aligning moment will result if the pneumatic trail is predicted correctly.

$$M_z = F_y x_{pt} \quad (8)$$

By using Equation 8 the relationship of the pneumatic trail could be determined by rearranging the equation and inputting the test data. It was seen that this equation could be represented by linear relationships. Consequently the two parameters of interest were the pneumatic trail gradient parameter ( $C_{xpt,\alpha}$ ) and the pneumatic trail intercept parameter ( $x_{pt,zero}$ ). These two parameters relate directly to the linear relationship determined to replicate the pneumatic trail response. As shown in Figure 12, these two parameters relate directly to the way in which the gradient and intercept values change and were also made load dependent.

To determine the pneumatic trail gradient and intercept parameters, the gradient and intercept values of the pneumatic trail responses for various vertical loads were taken and plotted against the vertical load. These plots yielded the relationships for the pneumatic trail gradient and intercept parameters. Consequently these relationships were used for the parameters where the gradient values of the relationships ( $C_{xpt,Fz}$  and  $x_{pt,zero,Fz}$ ) and intercept values ( $C_{xpt,INT}$  and  $x_{pt,zero,INT}$ ) were input to determine the main parameters; these relationships are summarised in Equations 9 and 10. The final formulation of pneumatic trail is given in Equation 11.

$$C_{xpt,\alpha} = C_{xpt,Fz} F_z + C_{xpt,INT} \quad (9)$$

$$x_{pt,zero} = x_{pt,zero,Fz} F_z + x_{pt,zero,INT} \quad (10)$$

$$x_{pt} = C_{xpt,\alpha} |\alpha| + x_{pt,zero} \quad (11)$$

To demonstrate the capability of the model, what follows is a comparison of the LPTM model with the aircraft test data. The model was set up using the established procedures without any subsequent refinement to the model parameters. The model was then used to calculate results which used the operational conditions seen within the test data i.e. the range of vertical loads and slip angles. The model results were then plotted against the aircraft test data and the results for the side force and aligning moment can be seen in Figures 13 and 14.

## 4 MODEL IMPLEMENTATION AND SIMULATION

For the model described here a technique known as the Control System Import Function provided with MSC ADAMS was used to import Mathworks Simulink models to control a particular aspect of a multi-body simulation, in this case the tyre model. The principle behind this technique is to allow the strengths of both ADAMS and Simulink to be combined into one modelling arena. It was known that this technique was primarily used to import hydraulic and control systems into ADAMS and that the potential for implementing tyre models through this methodology had not been explored. As a result the development of the new tyre model coincided with the development of the procedures required to implement the tyre model into the simulation environment.

To achieve this end, ADAMS and Simulink were set up so that a desired multi-body simulation was created within ADAMS while Simulink supplied the resulting information from the tyre model. The Control System Import Function was then utilised to combine the two components which closes the loop allowing the multi-body simulation to run. This process is illustrated for the two main stages of the process in Figures 15 and 16. The first stage is to set up ADAMS so that all of the operational information of the model can be passed to Simulink. This includes information such as the slip angle, tyre deflection and longitudinal velocity required in the tyre model to calculate the resulting forces and moment of interest. Additional, variables are also set up to pass the tyre forces and moments back into ADAMS from Simulink once they have been calculated. This information is then transported to Simulink where it can be attached to the tyre model via input and output ports which are simply created via standard flow diagrams. With this information defined, the Simulink model can be converted into C code in the form of a dll file.

Once created the dll file is then attached to the ADAMS multi-body model. The ADAMS model can then be solved as every integration step will send out the operational conditions which the dll file uses to calculate the ensuing tyre forces and moments and these are then passed back into ADAMS to allow the model to be solved.

Using this methodology, a number of simulation scenarios could be explored where the LPTM model in Simulink could be imported into ADAMS to allow a multi-body simulation to be performed. Examples of the simulations conducted are shown in Figure 17

where a virtual tyre test rig and nose landing gear model were created and run with the LPTM tyre model supplying the resulting tyre forces and moments of interest. The result of the implementation of this methodology leads to a means by which the model can be utilised in a number of simulation packages, which allows the introduction of the model into multiple simulation environments.

## 5 CONCLUSIONS

The work described here resulted in a new and unique low parameter tyre model specifically intended to replicate the aircraft tyres behaviour associated with aircraft manoeuvres on a runway. The results shown here are typical of those the model can achieve without any refinement to the parameters. The model is able to produce highly representative results when compared to the aircraft tyre test data whilst maintaining the low parameter ethos.

A methodology for the implementation of the model has been developed where the tyre model formulations exist in the Matlab/Simulink program. This allows the model to be transported to other simulation environments including the potential use with real time flight training simulators.

Overall the research has been able to provide a number of new alternatives when considering the simulation of aircraft tyres within a multi-body simulation environment from which further expansion of the model and simulation techniques are possible. In particular, the model has been shown to yield results which closely match that of the test data for the side force and self aligning moment and the formulations developed are readily amenable to accept the future modifications required to represent braking force.



## **Acknowledgements**

The authors would like to thank the staff within the Landing Gear Systems department at Airbus Operations Ltd (Filton). A particular thank you goes to Dr Wei Ding for his support during his time at Airbus. The authors would also like to acknowledge support from the Engineering and Physical Sciences Research Council.

## References

1. **Smiley, R.** Correlation, Evaluation, and Extension of Linearized, Theories for Tire Motion and Wheel Shimmy, *NACA-TM-Report 1299, USA, 1957.*
2. **Smiley, R. and Horne, W.** Mechanical Properties of Pneumatic Tires with Special Reference to Modern Aircraft Tires, *NASA Technical Report NASA-TR-64, Langley Research Centre, USA, 1960.*
3. **Gruber, P., Sharp, R.S. and Crocombe A.D.** Friction and camber influences on the static stiffness properties of a racing tyre, *Proc. IMechE Vol. 222 Part D: J. Automobile Engineering, DOI: 10.1243/09544070JAUTO872, 2008.*
4. **Bakker E., Nyborg L. & Pacejka, H.B.** Tyre modelling for use in vehicle dynamics studies, *SAE paper 870421, Society of Automotive Engineers, 400 Commonwealth Drive, Warrendale, PA 15096, USA, 1986.*
5. **Bakker E., Pacejka H.B. & Linder L.** A new tyre model with application in vehicle dynamics studies, *SAE paper 800087, 4th Auto Technologies Conference, Monte Carlo, 1989.*
6. **Pacejka H.B. & Bakker E.** The magic formula tyre model: tyre models for vehicle dynamic analysis, *Proc. 1st international colloquium on tyre models for vehicle dynamic analysis, ed. H. B. Pacejka, Swets & Zeitlinger, Lisse, 1993, pp. 1-18.*
7. **Fiala, E.** Seitenkrafte am rollenden Luftreifen, *VDI-Zeitschrift 96, 973, 1954.*
8. **Mechanical Dynamics Inc.** ADAMS/Tire (6.1) User's Manual, *Mechanical Dynamics Inc., 2301 Commonwealth Blvd., Ann Arbor, Michigan, USA, October 1992.*
9. **Daugherty, R.** A Study of the Mechanical Properties of Modern Radial Aircraft Tires, *NASA Technical Report NASA/TM-2003-212415, USA, 2003.*
10. **Ding W. and Sharma S.** Requirements for aircraft tyre models, *International Tire Technology Expo 2006, Stuttgart, March 2006, 2006.*

11. **Bridgestone Aircraft Tires**, [http://ap.bridgestone.co.jp/pdf/Tire\\_Specifications.pdf](http://ap.bridgestone.co.jp/pdf/Tire_Specifications.pdf), Site Accessed on 21st August 2010.
12. **Tanner, J. et al**, Static and Yawed-Rolling Mechanical Properties of Two Type VII Aircraft Tires, NASA Technical Paper 1863, May 1981
13. **Vogler, W. & Tanner, J.**, Cornering Characteristics of the Nose-Gear Tire of the Space Shuttle Orbiter, NASA Technical Paper 1917, 1981
14. **Daugherty, R.**, A Study of the Mechanical Properties of Modern Radial Aircraft Tires, *NASA Technical Report NASA/TM-2003-212415*, 2003
15. **Davis, P. et al**, Langley Aircraft Landing Dynamics Facility, NASA Reference Publication 1189, October 1987
16. **Carter, John & Nagy, Christopher**, The NASA Landing Gear Test Airplane, NASA Technical memorandum 4703, 1995
17. **Bridgestone Aircraft Tires**, For bias-ply tyres use [ap.bridgestone.co.jp/products/bias](http://ap.bridgestone.co.jp/products/bias) and for radial tyres use [ap.bridgestone.co.jp/products/radial](http://ap.bridgestone.co.jp/products/radial), Bridgestone Tyre Construction Descriptions, Internet source accessed on 17<sup>th</sup> March 2005
18. **MTS**, [www.mts.com/aesd/boeing\\_aircraftTire](http://www.mts.com/aesd/boeing_aircraftTire), Boeing Tyre Test Facilities, Internet source accessed on 19<sup>th</sup> October 2006
19. **Gipser, M.**, *FTire*: 10 Years of Development and Application, [http://www.cosin.eu/res/FTire\\_2008.pdf](http://www.cosin.eu/res/FTire_2008.pdf), Site Accessed on 21st August 2010
20. **Gipser, M.**, ADAMS/FTire - A Tire Model for Ride & Durability Simulations, [http://www.cosin.eu/res/ftire\\_eng\\_2.pdf](http://www.cosin.eu/res/ftire_eng_2.pdf), Site Accessed on 21st August 2010

21. **Sharp, R. & El-Nashar, A.**, A Generally Applicable Digital Computer Based Mathematical Model for the Generation of Shear Forces by Pneumatic Tyres, *Vehicle Systems Dynamics*, volume 15, pages 187-209, 1983
22. **Tsotras, A. & Mavros, G.**, The simulation of in-plane tyre model behaviour: a broad model range comparison between analytical and discretised modelling approaches, *Vehicle System Dynamics*, Volume 47, Issue 11 November 2009 , pages 1377 – 1400
23. **Tsotras, A. & Mavros, G.**, A model-based derivation of transient pressure distribution along the tyre-road contact, SAE 09AC-0070, 2009
24. **Yang, X. et al**, Materials Testing for Finite Element Tire Model, SAE International, 2010-01-0418, Published on 04/12/2010
25. **Ojala, J.**, Using ABAQUS in tire development process, ABAQUS Users' Conference 2005, Pawtucket, USA, October 14, 2004
26. **Alkan, V. et al**, Finite Modelling of Tyre Static Enveloping Characteristics, Proceedings of the Institute of Mechanical Engineers, Part C, Journal of Material Engineering Science, Journal Number JMES1753
27. **Gipser, M.** FTire, a New Fast Tire Model for Ride Comfort Analysis, *Proceedings of the 14<sup>th</sup> European ADAMS Users' Conference, Berlin (Germany), November 1999.*
28. **Vesimaki, Mauri** 3D Contact Algorithm for Tire-Road Interaction, *Proceedings of the 12<sup>th</sup> European ADAMS Users' Conference, Marburge Germany, November 1997.*
29. **Sharp, R. & El-Nashar, A.** A Generally Applicable Digital Computer Based Mathematical Model for the Generation of Shear Forces by Pneumatic Tyres, *Vehicle Systems Dynamics*, volume 15, pages 187-209, 1983.
30. **Hirschberg, Wolfgang et. al.** User-Appropriate Tyre-Modelling for Vehicle Dynamics in Standard and Limit Situations, *Vehicle Systems Dynamics*, Volume 38, Issue 2, Pages 103-125, 2002.

31. **Delft User Manual** MF-Tyre User Manual Version 4.3, *Developed by TNO Road-Vehicle Research Institute, 1995.*
32. **Blundell M. V.** A low parameter tyre model for handling simulation, *The 4<sup>th</sup> European Conference for Tire Design and Manufacturing Technology, Stuttgart, Germany, March 2004.*
33. **Milliken, William & Milliken, Douglas** Race Car Vehicle Dynamics, *USA (Warrendale), SAE International 1995.*
34. **Gim, Gwanghun & Choi, Youngchul** Improved UA tire model as a semi-empirical model, *Seoul 2000 FISTA World Automotive Congress, June 12-15, Seoul, Korea, 2002.*
35. **ADAMS 5.2.1 Guide** (1989), ADAMS/Tire User's Guide, *Release 6.0 of ADAMS//Tire User Guides, Mechanical Dynamics Incorporated, Michigan USA, 1989.*
36. **Tanner, J. et al** Mechanical Properties of Radial-Ply Aircraft Tires, *SAE 2005-01-3438, USA, SAE International, 2005.*
37. **Blundell M. V. and Harty, D.** The Multibody Systems Approach to Vehicle Dynamics, *Elsevier Science, June 2004.*

## Figure Captions

- Figure 1: Speed Dynamics Machine for Tyre Testing Formerly at Dunlop Tyres Ltd.
- Figure 2: Landing Gears and Tyres (courtesy of Airbus Operations Ltd)
- Figure 3: Airbus TERATYRE (Test Rig for Aircraft TYRE) Machine [10]
- Figure 4: Available Aircraft Tyre Data versus Current Need (adapted from [10])
- Figure 5: Examples of a Finite Element Aircraft Tyre
- Figure 6: The SAE Tyre Coordinate System used by the LPTM Tyre Model
- Figure 7: Side Force with Slip Angle (Fiala Model and Test Data)
- Figure 8: Side Force with Slip Angle (Harty Model and Test Data)
- Figure 9: Self Aligning Moment with Slip Angle (Fiala Model and Test Data)
- Figure 10: Self Aligning Moment with Slip Angle (Harty Model and Test Data)
- Figure 11: Side Force Response Breakdown
- Figure 12: Pneumatic trail gradient and intercept parameter definitions
- Figure 13: Side Force with Slip Angle (LPTM Model and Test Data)
- Figure 14: Self Aligning Moment with Slip Angle (LPTM Model and Test Data)
- Figure 15: Stage 1 of the Control System Import Function methodology
- Figure 16: Stage 2 of the Control System Import Function methodology
- Figure 17: ADAMS Models Developed Utilising the Control System Import Function

## Table Captions

- Table 1: Examples of Available Tyre Models

Application	Tyre Model	Model Type	Specifically for Automotive	Adapted for Aircraft	Specifically for Aircraft
Durability / Vehicle Handling Studies	ADAMS Durability [28]	Physical	●		
	FTire [27]	Physical	●	●	
	Sharp [29]	Physical	●		
	TM Easy [30]	Empirical	●		
Vehicle Handling Studies	Daugherty [9]	Empirical			●
	Delft [31]	Empirical	●		
	Fiala [7]	Empirical	●	●	
	Harty [32]	Empirical	●		
	Magic Formula [5]	Empirical	●		
	Magic Formula V3 [6]	Empirical	●		
	Milliken [33]	Empirical	●		
	NASA R-64 [2]	Empirical			●
	UA [34]	Empirical	●	●	
	ADAMS 5.21 [35]	Interpolation	●		

Table 1: Examples of Available Tyre Models

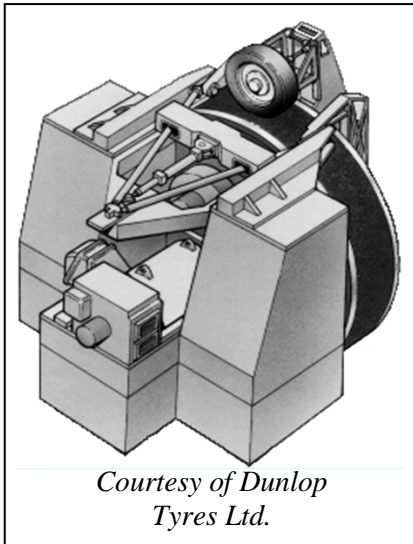


Figure 1: Speed Dynamics Machine for Tyre Testing Formerly at Dunlop Tyres Ltd.





Figure 2: Landing Gears and Tyres (courtesy of Airbus Operations Ltd)



Figure 3: Airbus TERATYRE (Test Rig for Aircraft TYRE) Machine [10]

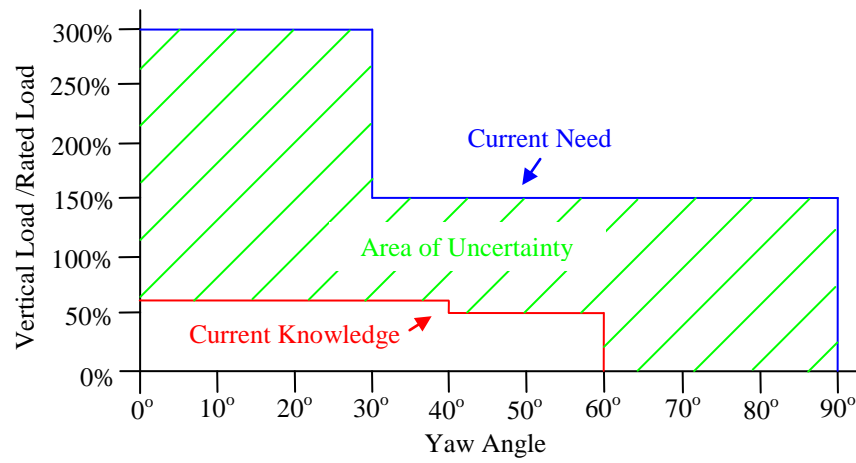


Figure 4: Available Aircraft Tyre Data versus Current Need (adapted from [10])

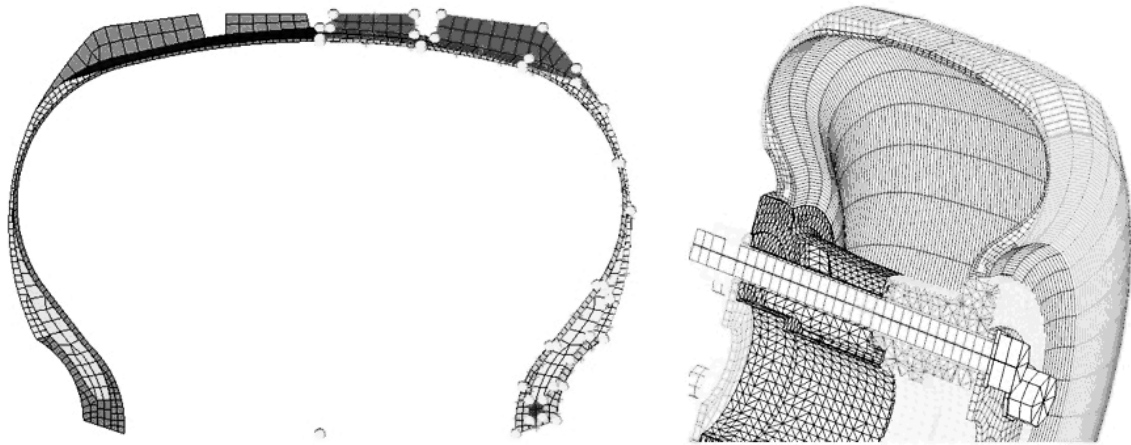


Figure 5: Examples of a Finite Element Aircraft Tyre

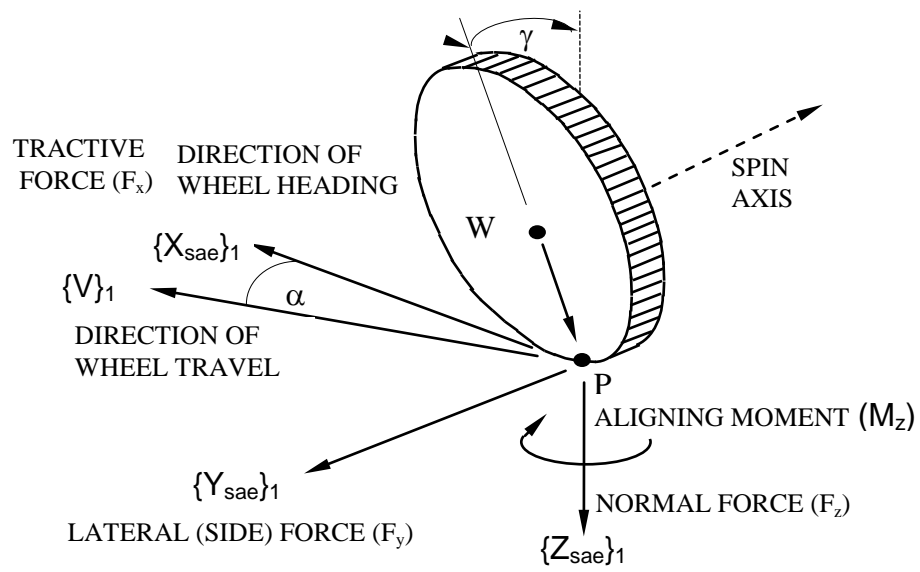


Figure 6: The SAE Tyre Coordinate System used by the LPTM Tyre Model

**Side Force Comparison Between Fiala Tyre Model Results  
and Aircraft Test Data**

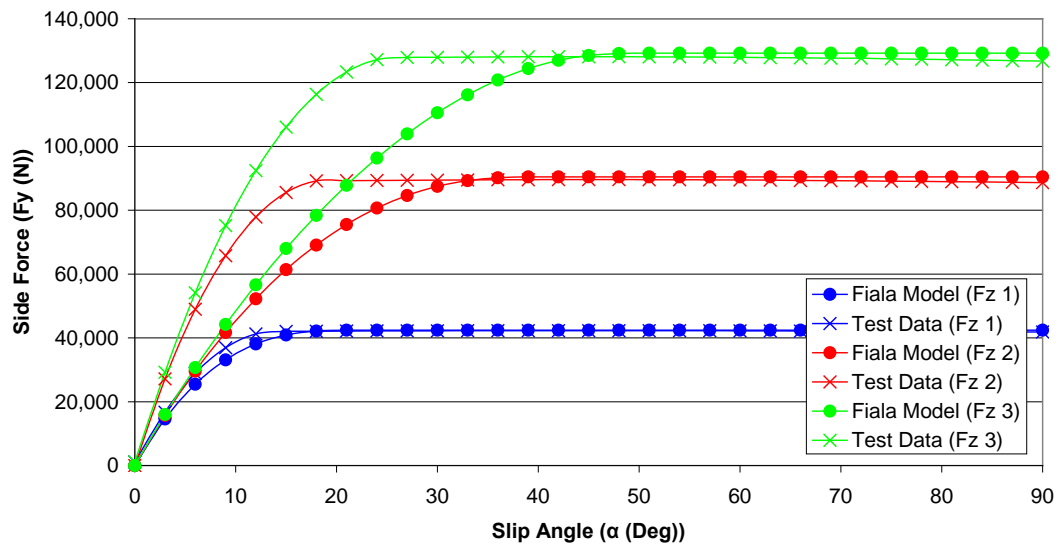


Figure 7: Side Force with Slip Angle (Fiala Model and Test Data)

**Side Force Comparison Between Harty Tyre Model Results  
and Aircraft Tyre Test Data**

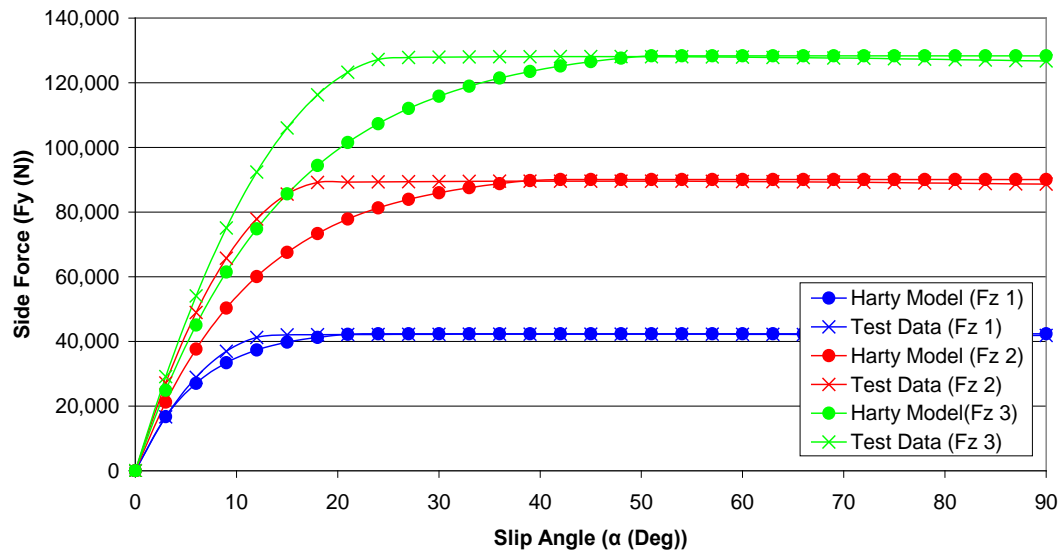


Figure 8: Side Force with Slip Angle (Harty Model and Test Data)

**Self Aligning Moment Comparison of Fiala Tyre Model Results  
and Aircraft Tyre Test Data**

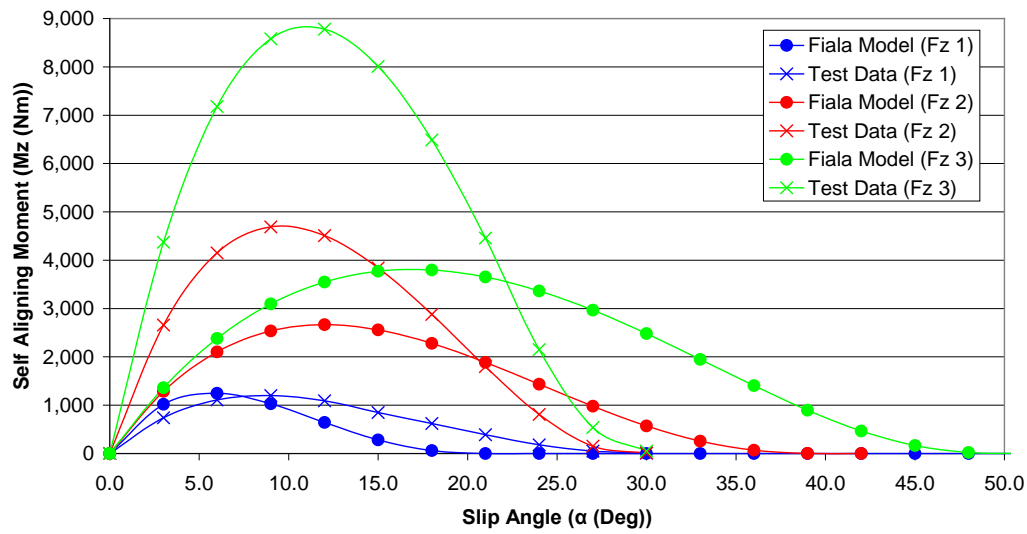


Figure 9: Self Aligning Moment with Slip Angle (Fiala Model and Test Data)



**Self Aligning Moment Comparison to Harty Tyre Model Results  
and Aircraft Tyre Test Data**

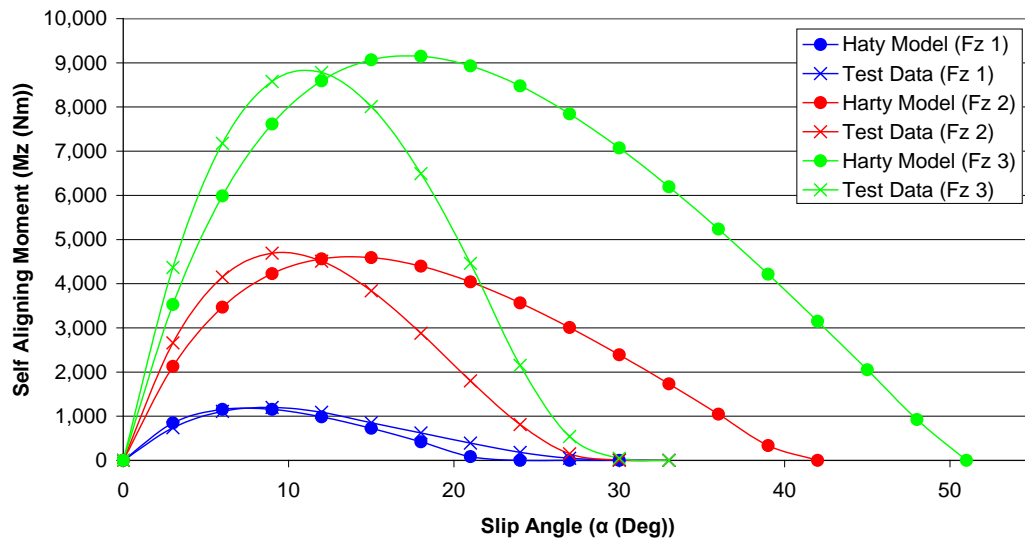


Figure 10: Self Aligning Moment with Slip Angle (Harty Model and Test Data)

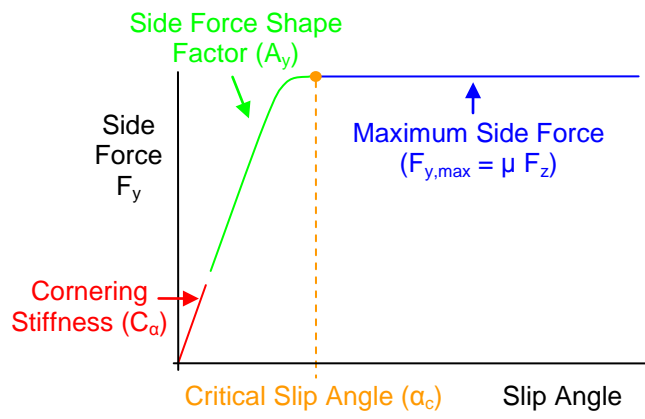
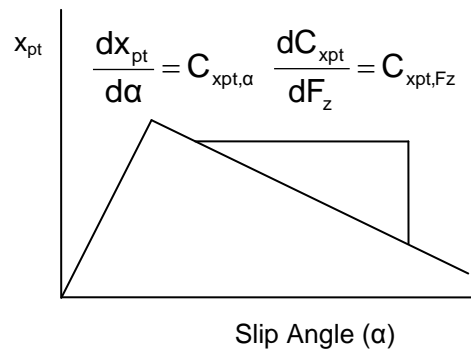


Figure 11: Side Force Response Breakdown

### Pneumatic trail Gradient Parameter



### Pneumatic Trail Intercept Parameter

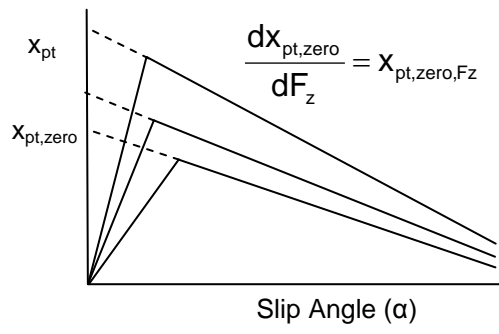


Figure 12: Pneumatic trail gradient and intercept parameter definitions

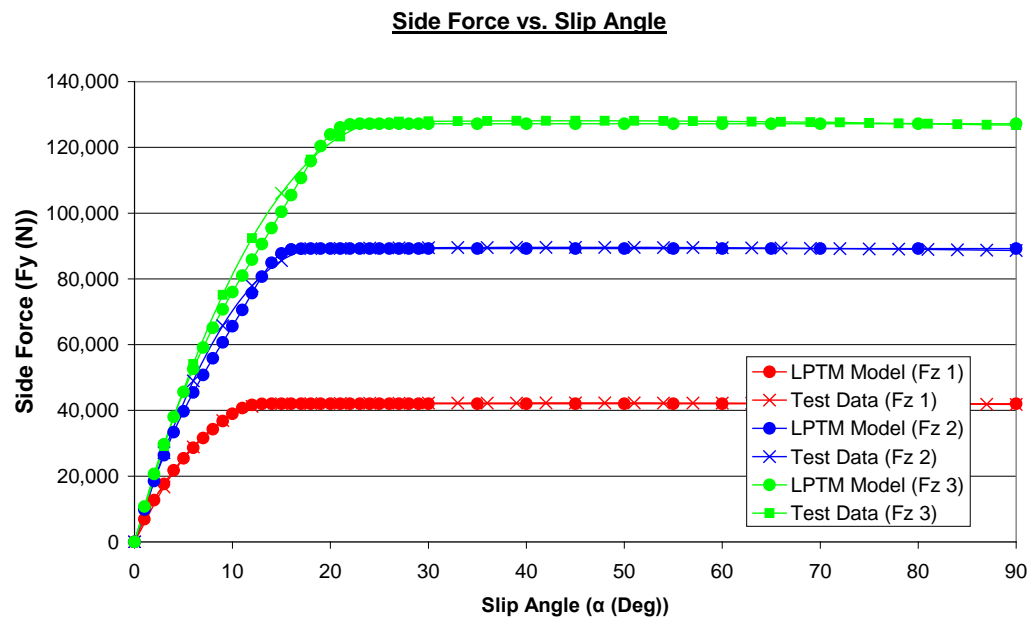


Figure 13: Side Force with Slip Angle (LPTM Model and Test Data)

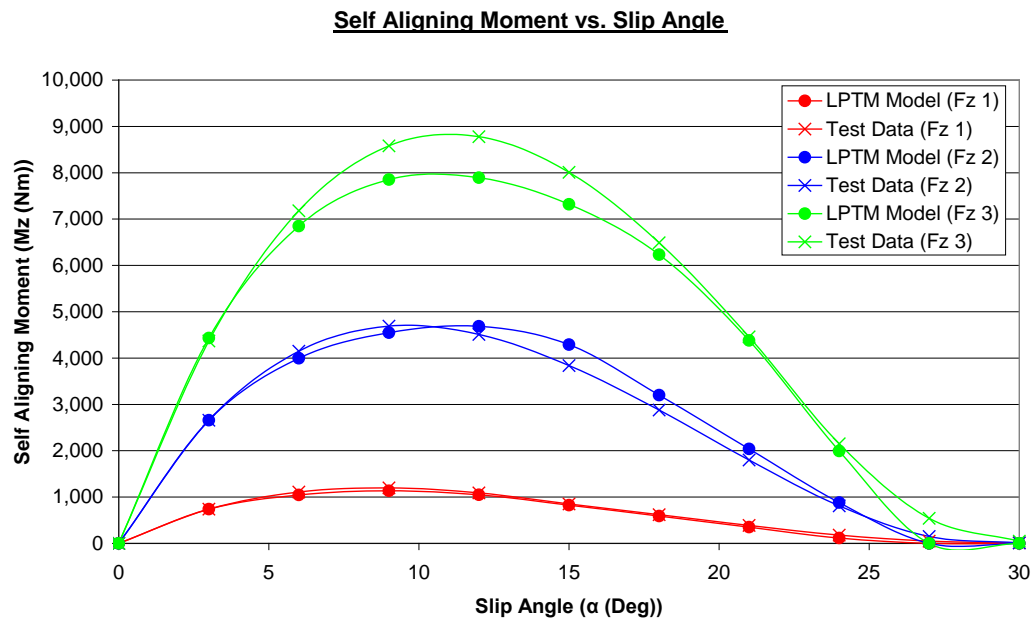


Figure 14: Self Aligning Moment with Slip Angle (LPTM Model and Test Data)

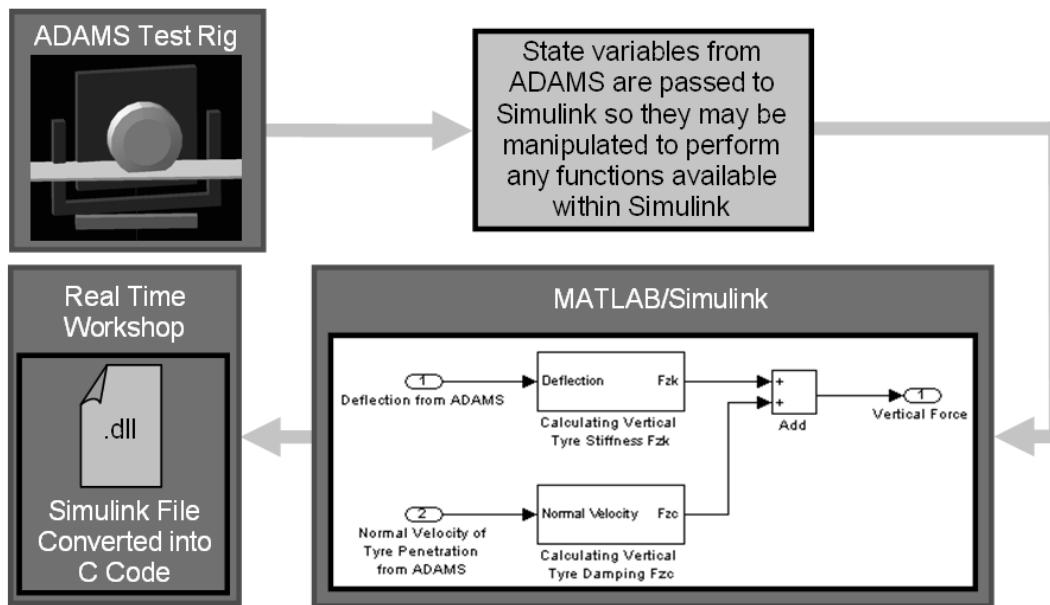


Figure 15: Stage 1 of the Control System Import Function methodology

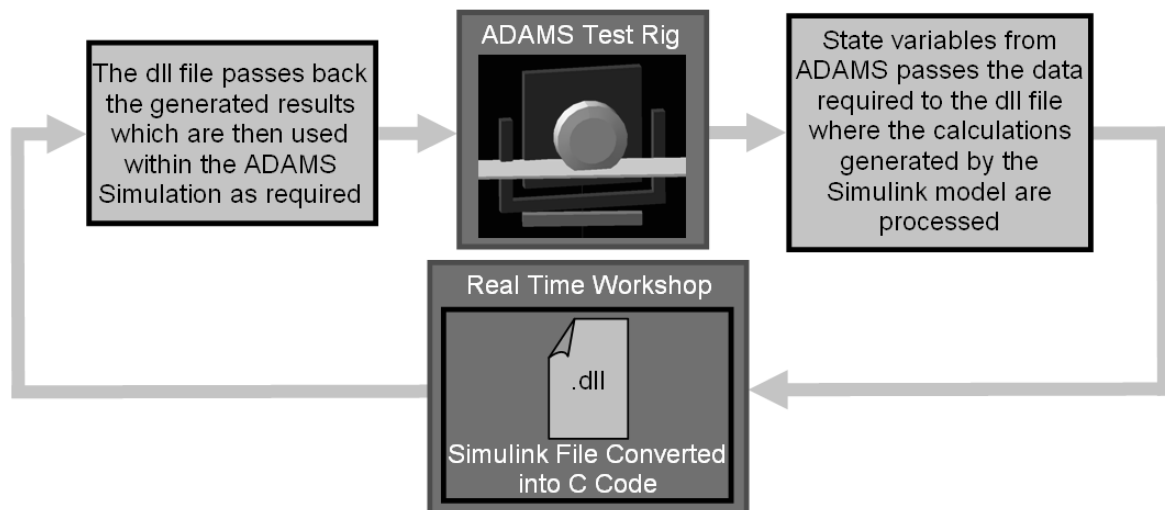


Figure 16: Stage 2 of the Control System Import Function methodology

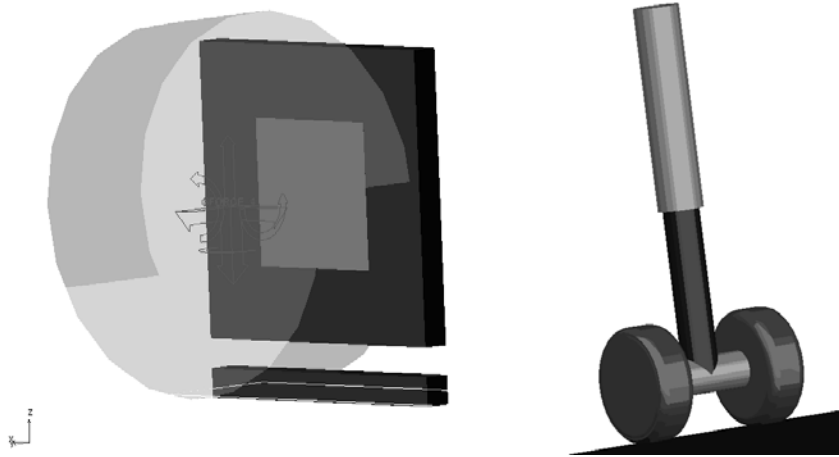


Figure 17: ADAMS Models Developed Utilising the Control System Import Function